JCTC Journal of Chemical Theory and Computation

ARTICLE

pubs.acs.org/JCTC

Hybrid QM/MM Calculations on the First Redox Step of the Catalytic Cycle of Bovine Glutathione Peroxidase GPX1

Juraj Kóňa*,† and Walter M. F. Fabian‡

†Institute of Chemistry, Center for Glycomics, Slovak Academy of Sciences, Dúbravska cesta 9, 845 38 Bratislava, Slovak Republic

‡Institute of Chemistry, Karl Franzens University, Graz, Heinrichstrasse 28, A-8010 Graz, Austria

Supporting Information

ABSTRACT: The first reaction step of the redox cycle of bovine erythrocyte glutathione peroxidase from class 1 (GPX1) was investigated using hybrid quantum mechanics/molecular mechanics (QM/MM) calculations using the ONIOM methodology. The reduction of hydrogen peroxide by the active-site selenocysteine in selenolate form assisted by the Arg177 residue was modeled based on a proposal from previous molecular dynamics simulations and pK_a calculations (*J. Chem. Theory Comput.* **2010**, *6*, 1670−1681). The redox reaction is predicted as a concerted S_N2 nucleophilic substitution with a concomitant proton transfer from Arg177 onto leaving hydroxide ion upon reduction of hydrogen peroxide. The height of the reaction barrier was predicted in range of 6−11 kcal mol^{-1}, consistent with an experimental rate constant of ca. 10^7 M^{-1} s^{-1}. The proposed GPX1-Se$^-$-Arg177H$^+$ mechanism for GPX1 is compared with the GPX3-SeH-Gln83 one proposed for human glutathione peroxidase from class 3 (GPX3) and with the solvent-assisted proton exchange mechanism proposed for GPX-like organic selenols. The structural and energetic parameters predicted by various density functional theory methods (B3LYP, MPW1PW91, MPW1K, BB1K, M05-2X, M06-2X, and M06) are also discussed.

1. INTRODUCTION

Glutathione peroxidase from class 1 (GPX1, EC 1.11.1.9) is a selenoprotein[1] which protects cells from oxidative damage by catalyzing the reduction of H_2O_2, lipidhydroperoxides, and other organic hydroperoxides using a selenocysteine residue (Sec) and glutathione (GSH, γ-glutamylcysteinylglycine) as a reducing substrate. A general scheme of the overall catalytic cycle is shown in Figure 1a. It has been experimentally suggested that the catalytically active form of the enzyme is the selenolate anion (E-Se$^-$).[2,3] In the first redox step, E-Se$^-$ is oxidized to the selenenic acid (E-SeOH) with the accompanying reduction of a hydroperoxide substrate to a corresponding alcohol (or water in the case of hydrogen peroxide) with an experimentally measured[4] rate constant of 4.1 × 10^7 M^{-1} s^{-1}. In the second step, the E-SeOH reacts with GSH to produce a selanyl sulfide adduct (E-SeSG). In the third step, a second molecule of GSH attacks E-SeSG to regenerate the active reduced form of the enzyme, and the oxidized form of GSH (GSSG) is formed as a byproduct. This step is the rate-determining step of the overall mechanism with a rate constant of 2.3−5.1 × 10^5 M^{-1} s^{-1}.[4,5] As it can be seen in the reaction scheme (Figure 1a), a proton must be supplied for the first redox step and be abstracted in the third reaction step to maintain overall stoichiometry of the catalytic process. The mode of action of these proton transfers is not clear because no ionizable amino acid residues were found in the proximity of the Sec reaction center in available X-ray structures of GPX1[2,6] and other glutathione peroxidases.[7−10] The active site is characterized by the highly conserved Sec-Trp-Gln triad, however, five ionizing residues (Arg50, 96, 177, and 178 and His79) do place in the active site with a radius of 6−12 Å from Sec45 in GPX1 (PDB ID: 1GP1).[2] A similar situation occurs in other glutathione peroxidases, e.g., for human plasma glutathione peroxidase 3 (GPX3), six ionizing residues (Arg123, 168, 180, and 201, Lys106, and His200) can be found within a radius of 12 Å around Sec73 (PDB ID: 2R37).[7,10] It is supposed that these residues influence the catalytic process and are involved in specific binding of GSH.[2,7,11] Molecular dynamics (MD) simulations on GPX1 indicated that side chains of Arg177 or His79 can approach to proximity of Sec45, thus, possibly acting as the acid/basic catalyst in reduction of peroxides by GPX1 (the GPX1-Se$^-$-Arg177H$^+$ mechanism in Figure 1c).[11] A chemical role of arginine as an acid catalyst in the redox reactions of GPX1 (or GPX3) has not been verified yet. Recently, a mechanism based on the solvent-assisted proton exchange (SAPE) was proposed for redox reactions of GPX-like organoselenium compounds[12−15] and for human plasma GPX3[16−18] using quantum mechanics (QM) calculations. In the proposed mechanism for GPX3[16] (Figure 1b) water molecules participate in proton exchange between the selenol (and thiol groups) of selenocysteine [and thioredoxin (TRX)] and the amide groups of protein amino acids. It is based on the assumption that nonionizing Gln83 (side chain amide nitrogen) and Leu51 (backbone amide nitrogen) play roles of catalytic bases, and the active reduced form of Sec is selenol rather than selenolate. The calculated reaction barriers of the GPX3 mechanism (GPX3-Se$^-$-H_2O-Gln83H$^+$, SeH-Gln83, and GPX3-Se$^-$-H_2O-Leu51H$^+$) are in the range of 17−22 kcal mol^{-1} and correspond to chemical reactions of ca. 10^7 times slower, as it was found in the experimental measurements.[4,5] The calculated barriers in that work[16,17] are in good agreement with benchmark calculations[14] for GPX-like organoselenium compounds, indicating that a more favorable scenario of the redox mechanism of GPX3 and other glutathione

Received: February 22, 2011
Published: June 14, 2011

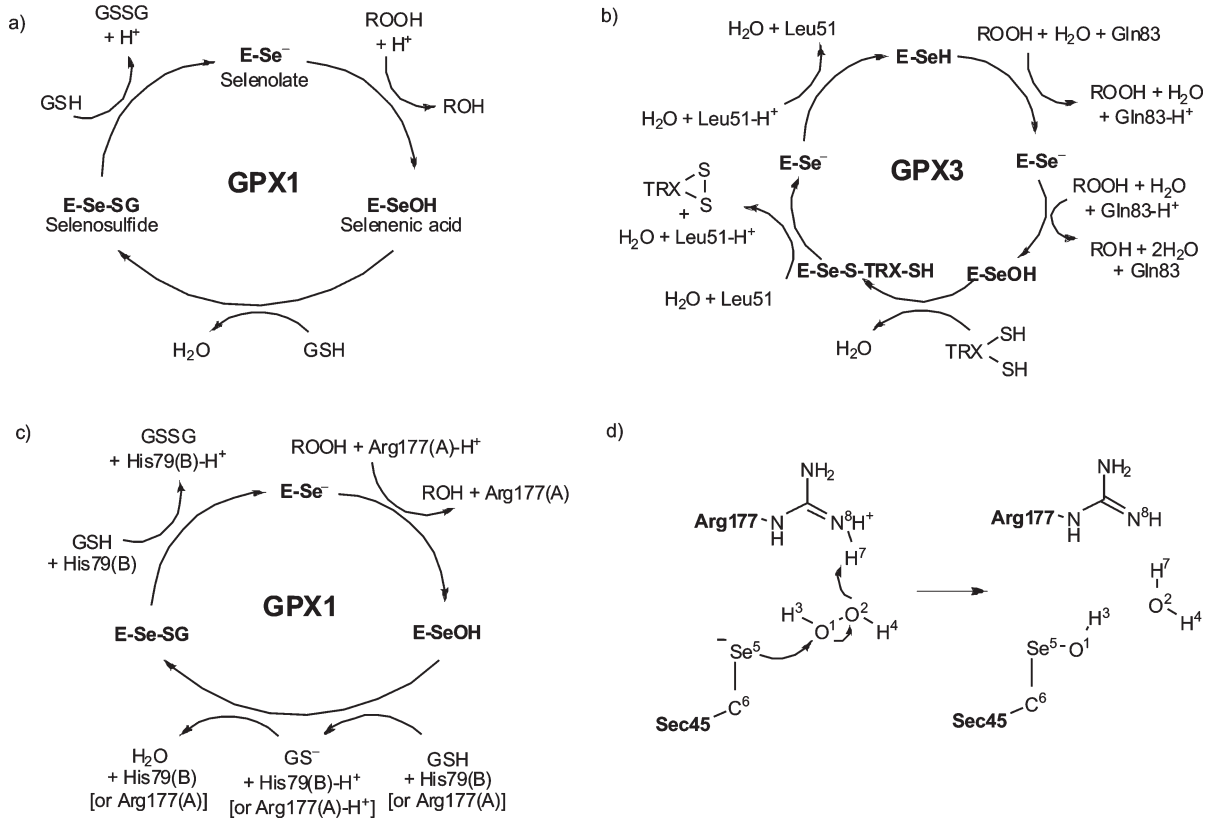

Figure 1. (a) A general scheme for the catalytic cycle of GPX1 after Epp et al.[2] The resting state of Sec is selenolate. A proton donor and acceptor in the first and third redox steps are not known. (b) A catalytic mechanism proposed for GPX3 by Prabhakar et al.[16] based on DFT calculations. The resting state of Sec is selenol. The concomitant proton transfers occur between Sec and amide nitrogen of Gln83 and between TRX and amide nitrogen of Leu51 facilitated by solvent water molecules. (c) A proposed catalytic mechanism of GPX1 by Ali et al.[11] of which the first redox step is calculated at the hybrid QM/MM level in this work. (d) The calculated reaction step with the atom numbering.

peroxidases, consistent with the experimental rate[4,5] of 2.3–5.1 × 10^5 M^{-1} s^{-1}, could be operative. The proposed GPX3 mechanism[16,17] has the reaction barriers comparable to those calculated for the redox reactions in the gas phase and in aqueous solution rather than in the enzyme.[12−15,19−23] Indeed, the QM calculations on the redox reactions of selenols and thiols without assistance of the proton exchange catalyst predicted unreasonably high reactions barriers.[24−26]

Here we modeled the first reaction step of the redox cycle of bovine GPX1 based on the proposed GPX1-Se^--Arg177H^+ mechanism (Figure 1c) from the previous MD simulations and pK_a calculations[11] using density functional theory (DFT) methods. We will show that the mechanism with the selenolate form of Sec45 and a direct participation of a weak acid or base, in our case Arg177, in the reduction of hydrogen peroxide has a reaction barrier consistent with an experimental rate constant measured for this reaction step in human GPX1 and is energetically favorable over the GPX3-Se^--H_2O-Gln83H^+,[27] GPX3-SeH-Gln83,[28] and the SAPE mechanisms.[12−15] We will also briefly discuss inaccuracies in the prediction of the reaction barrier calculated with three hybrid (B3LYP, MPW1PW91, MPW1K) and four meta-hybrid functionals (BB1K, M05-2X, M06-2X, and M06).

2. COMPUTATIONAL DETAILS

The reaction mechanism of the first redox step was calculated using an enzyme model, which consisted of the structure of GPX1, enzyme substrate (H_2O_2), and explicit solvent molecules (water cap around the active-site Sec45 consisted of 246 water molecules). The structure of GPX1 and water was built from a snapshot selected from a trajectory calculated in the previous MD simulations[11] based on the crystal structure of bovine GPX1 (PDB ID: 1GP1).[2] The GPX1 embedded in a box with water molecules was equilibrated 4 ns in the MD simulation with selenolate redox state (E-Se^-) without a substrate and a glutathione cofactor. Then, in a selected snapshot all water molecules except those located around Sec45 (up to ca. 15 Å) were deleted, and the structure was subsequently minimized without any constrains at the molecular mechanics (MM) level prior to quantum mechanics/molecular mechanics (QM/MM) calculations. The ionization states of the ionizing amino acid residues of the enzyme were predicted by the PropKa program[27] considering an in vivo pH of 7.

Transition states and corresponding intermediates of the reaction were optimized at the hybrid QM/MM level with the ONIOM methodology[28] with the mechanic embedding scheme (ONIOM-ME-DFT/6-31G(d,p):Amber)[17,18] using the Gaussian 09 package[29] (Gaussian inputs of the MPW1PW91 optimized geometries are available in Supporting Information). The electrostatic effects of the enzyme were evaluated with the electronic embedding (ONIOM-EE) scheme by single point energy calculations on optimized structures in the ONIOM-ME scheme (ONIOM-EE-DFT/6-311+G(3df,2p):Amber//ONIOM-ME-DFT/6-31G(d,p):Amber). We used for the optimization the

ONIOM-ME scheme since optimization of GPX3 with the ONIOM-EE scheme did not improve the results and gave a slightly larger rms deviation when the ONIOM-EE geometries were compared with the X-ray structure of the enzyme.[18] For the QM part of the ONIOM model (Sec45, Gly46, side chain of Thr47 without a methyl group, side chains of Gln80, Trp158, and Arg177, 3 molecules of H_2O located around the Sec45 residue, and the substrate H_2O_2), various DFT functionals were used: The hybrid generalized gradient approximation (GGA) Becke exchange functional with the Lee−Yang−Parr correlation functional (B3LYP),[30,31] the modified Perdew−Wang exchange functional combined with the Perdew−Wang-1991 correlation functional (MPW1PW91),[32,33] MPW1PW91 modified for kinetics (MPW1K),[34] the meta-hybrid GGA Becke88-Becke95 1-parameter for kinetics (BB1K),[35] and Minnesota functionals with double the amount of nonlocal exchange (M05-2X[36] and M06-2X)[37] as well as meta-hybrid GGA M06 functional.[37] In addition, the second-order Møller−Plesset theory (MP2)[38,39] method was used for single point energy calculations on the optimized B3LYP, MPW1PW91, and MPW1K structures using the ONIOM-EE and ONIOM-ME schemes and the Pople's split valence triple-ζ basis set augmented by diffuse and polarization functions [6-311+G(3df,2p)]. The MM part of the system was treated with the standard AMBER[40] (enzyme) and TIP3P[41] (water) force fields. For H_2O_2, selenolate (Sec45-Se^-) and selenenic acid (Sec45-SeOH) redox forms of selenocysteine parameters were derived either from the AMBER and GAFF force fields or built from data obtained by ab initio Hartree−Fock calculations[42] [HF/6-31G(d)] using the Gaussian 09 package.[29] Atom types, charges, and added force field parameters are provided in Supporting Information. The electrostatic potential fitting algorithm of the Merz−Singh−Kollman scheme[43] was used to estimate atomic charges from the HF/6-31G(d) calculations.

All stationary points were characterized as minima or as transition states by vibrational frequency calculations. Transition states were verified as having one and only one imaginary frequency. In addition, for each transition state, intrinsic reaction coordinate (IRC) calculations were performed to confirm that it connects the correct reactant and product minima. Thermodynamic quantities were calculated at 298 K and 101 325 kPa using standard rigid rotor and harmonic oscillator partition function expressions. Zero-point and thermal corrections to enthalpy and Gibbs free energies were calculated from unscaled frequencies obtained at the same level as the geometry optimizations.

The stability of wave function of the transition state in calculations with the restricted HF formalism was tested with the unrestricted MP2 and B3LYP calculations. We found for both methods no differences in energies; therefore, all calculations in this work were performed with the restricted formalism.

3. RESULTS AND DISCUSSION

In the first part we describe and discuss results obtained by the B3LYP and MPW1PW91 functionals in order to compare structural and energetic parameters with those calculated by the same functionals for GPX3[16,17] and organic selenols.[12−14] Then, we will discuss structural and energetic differences found among seven functionals.

3.1. Redox Mechanism GPX1-Se^--Arg177H^+. Based on scan calculations along the Se^5-O^1 reaction coordinate (for atom numbering see Figure 1d) at the B3LYP/6-31G(d,p) level, a preliminary structure of a transition state was obtained. By subsequent transition-state optimization, the structure of **TS12** was localized at a distance $d(Se^5-O^1)$ = 2.52 Å (B3LYP) and 2.43 Å (MPW1PW91) (Table 1 and Figure 2). The **TS12** was verified by vibrational frequency calculations with one large imaginary frequency [ν_i = 286i (B3LYP) and 355i cm^{-1} (MPW1PW91)] belonging to the breaking−forming bonds (O^1-O^2, Se^5-O^1, and O^2-H^7). The IRC calculations started from **TS12** resulted in a Michaelis complex **1** and a selenenic acid intermediate **2**. The reaction path **1** → **TS12** → **2** is predicted by the hybrid QM/MM methodology as a general acid-catalyzed nucleophilic substitution proceeding by the S_N2 mechanism, in which addition of the nucleophile (selenolate ion of Sec45-Se^-), elimination of the leaving group (hydroxide ion from the hydrogen peroxide substrate), and proton transfer from the acid catalyst (Arg177−H^+) onto the leaving group take place in a concerted manner [$d(Se^5-O^1)$ = 2.52 Å, $d(O^1-O^2)$ = 1.71 Å, $d(O^2-H^7)$ = 1.87 Å, and $d(H^7-N^8)$ = 1.04 Å (B3LYP)]. The proton transfer significantly lags behind the breaking of the O^1-O^2 bond of the substrate, indicating mainly its role in stabilization of the formed byproduct (H_2O) rather than in facilitating the departure of the leaving group in the transition state. When we compared pK_a values of arginine (12.5), the forming selenenic acid intermediate (12.0),[22] and the byproduct H_2O (15.7), the proton transfer Arg177−H^+ + OH^- → Arg177 + H_2O would be only slightly preferred compared to Sec45-SeOH + OH^- → Sec45−O^- + H_2O. However, the geometry of **TS12** disfavors the direct proton transfer from Sec45-SeOH onto OH^-. In **TS12**, the value of the angle between the nucleophile selenium atom, the reaction oxygen center, and the leaving group approaches 180° [$\phi(Se^5-O^1-O^2)$ = 172.59° (B3LYP) and 173.1° (MPW1PW91)]. Thus, the position of the atoms is more optimal for transfer of H^7 from Arg177 than for H^3 from H_2O_2 to OH^- [also $d(O^2-H^7)$ = 1.87 Å is shorter than $d(O^2-H^3)$ = 2.06 Å (B3LYP)]. It is known from the other QM calculations[19,21,24−26] performed for the reaction of selenols with hydroperoxides without a proton exchange catalyst, that the leaving hydroxide ion has to abstract a proton directly from the oxygen of the forming selenenic acid. Thus, in the transition state the Se−O−O linear structure is deformed to a more bent geometry [for example, ϕ(Se−O−O) = 73−112°,[24] 82−138°,[26] or 164°].[19]

The longer distance $d(Se^5-O^1)$ = 2.52 Å (B3LYP) and 2.43 Å (MPW1PW91) compared with TS geometries of selenols with the SAPE mechanism [d(Se−O) = 2.14 Å (MPW1PW91)][12] indicates an earlier transition state when Sec45 is in the selenolate form, and the acid catalyst directly participates in the redox process.

Our best prediction of the thermochemical kinetics parameters, including larger basis set [6-311+G(3df,2p)] and electrostatic effects of the enzyme (ONIOM-EE), is 11.0 kcal mol^{-1} (MPW1PW91), 11.2 kcal mol^{-1} (M06), and 6.0 kcal mol^{-1} (B3LYP) for the activation free energy ($\Delta G^{\ddagger}$) and −24.2, −31.5, and −23.8 kcal mol^{-1} for the reaction energy (ΔG_r, Table 3). These values were further validated using the MP2 method as an ab initio reference method. Under assumption that DFT methods used in this work have an average error of 2−5 kcal mol^{-1} for the reaction barriers,[34−37,44−47] the results correlate quite well with the MP2 ones, where values of $\Delta G^{\ddagger}$ = 8.4 kcal mol^{-1} (MP2//MPW1PW91) and 8.3 kcal mol^{-1} (MP2//B3LYP) were predicted (Figure 3). They also reasonably converge to an experimentally measured rate constant for the first redox step of human GPX1 ($\Delta G_{exp}^{\ddagger}$ of ca. 7 kcal mol^{-1} can be estimated from k_{exp} = 4.1 × 10^7 M^{-1} s^{-1}).[4]

Table 1. Selected Geometry Parameters, Interatomic Distances (d) (in Å), Valence (φ), and Torsion angles (Φ) (°) of the Optimized Transition States and Intermediates at the Various DFT Levels Using the ONIOM-ME-DFT/6-31G(d,p):Amber Methodology.[a]

	$d(Se^5-O^1)$	$d(O^1-O^2)$	$d(O^2-H^7)$	$d(H^7-N^8)$	$d(O^2-H^3)$	$\varphi(C^6-Se^5-O^1)$	$\varphi(Se^5-O^1-O^2)$	$\Phi(C^6-Se^5-O^1-O^2)$
					B3LYP			
1	3.085	1.449	2.133	1.021	1.940	117.21	121.14	−125.71
TS12	2.523	1.713	1.868	1.035	2.060	107.14	172.59	162.69
2	1.833	2.631	1.028	1.655	1.846	98.02	140.26	−127.81
					MPW1PW91			
1	3.057	1.427	2.107	1.018	1.923	117.40	120.81	−126.96
TS12	2.426	1.729	1.812	1.036	2.043	107.29	173.09	166.43
2	1.814	2.609	1.031	1.613	1.813	98.15	139.46	−128.75
					MPW1K			
1	3.063	1.406	2.064	1.013	1.898	117.12	120.37	−129.27
TS12	2.339	1.752	1.776	1.032	2.019	107.18	173.17	166.09
2	1.818	2.631	1.000	1.698	1.848	94.51	139.79	−131.26
					BB1K			
1	3.117	1.411	2.069	1.013	1.894	114.74	119.11	−135.31
TS12	2.350	1.756	1.802	1.029	2.030	107.23	173.83	163.74
2	1.821	2.664	0.995	1.736	1.871	94.67	137.68	−128.32
					M05-2X			
1	3.132	1.422	2.041	1.016	1.906	113.02	119.78	−137.91
TS12	2.310	1.781	1.785	1.036	2.034	107.35	172.62	151.39
2	1.827	2.636	1.037	1.600	1.776	94.798	131.71	−130.60
					M06-2X			
1	3.142	1.422	1.998	1.022	1.908	111.03	119.47	−141.71
TS12	2.317	1.778	1.760	1.041	2.043	107.08	172.11	142.55
2	1.825	2.636	1.028	1.626	1.796	94.791	132.95	−129.57
					M06			
1	3.127	1.423	2.035	1.024	1.908	115.13	119.77	−132.41
TS12	2.461	1.724	1.837	1.036	2.054	109.73	169.28	147.61
2	1.827	2.676	1.010	1.727	2.811	95.44	139.81	−125.58

[a] For atom numbering see Figure 1d.

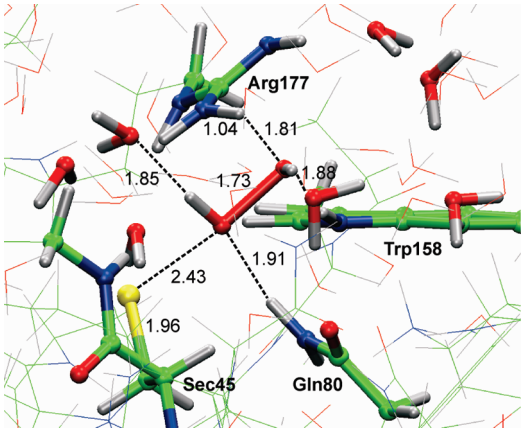

Figure 2. The MPW1PW91 optimized transition state **TS12** with selected distances (in Å) (selenium is in yellow, carbons in green, nitrogens in blue, oxygens in red, and hydrogens in gray).

The calculated mechanism with the GPX1-Se^--Arg177H^+ dyad has the reaction barrier ca. 7−8 kcal mol^{-1} lower compared with those calculated for the first redox step of GPX3 with the GPX3-SeH-Gln83 dyad [18.0 kcal mol^{-1}, ONIOM-ME-B3LYP/6-311+(d,p):Amber//ONIOM-ME-B3LYP/6-31G-(d):Amber][17] or the SAPE mechanism E-Se^--H_2O-Gln83-H^+ [17.1 kcal mol^{-1}, IEF-PCM-B3LYP/6-311+G(d,p)//B3LYP/6-31G(d)].[16] For the sake of clarity, we compare the ONIOM-ME results (Table 2) since the mechanism with the GPX3-SeH-Gln83 dyad[17] was not performed with the ONIOM-EE methodology. Based on the previous experimental study[3] and pK_a calculations for selenocysteine in GPX1[11] and in water,[48] Sec45 can be in either selenol or selenolate form, with the preferable selenolate form in physiological pH. Our calculations on the first redox step of GPX1 further support selenolate as the resting reduced state of GPX1. We show that if a weak acid or base (roughly said a catalyst with pK_a > 7) can directly participate in proton exchange with a hydroperoxide substrate, the redox step can proceed very fast with a rate of ca. 10^7 s^{-1}.

The SAPE mechanism proposed by Bayse and Antony[12−15] has not been tested yet for any enzyme GPX system at the QM/MM level, but it is plausible mainly for the redox reaction of organic selenol converted to selenenic acid in absence of an acidic

or basic catalyst in aprotic solvents, e.g., the reaction of selenol in tetrahydrofuran[49] or dichloromethane[50] where a catalytic amount of water needed for the SAPE process is produced as a byproduct in the reduction of hydroperoxide substrate. Indeed, the reaction barriers for the SAPE mechanism[12−15] in the range of 19−22 kcal mol^{-1} are comparable to the proposed GPX3-SeH-Gln83 mechanism but 2−3 times higher compared with the GPX1-Se$^-$-Arg177H$^+$ mechanism investigated in this work. Clearly, the GPX1 could catalyze the reduction of hydroperoxides in the resting selenol form, as an alternative when the selenolate form is not available, but this reaction would proceed only slowly with a rate of ca. 10^{-2} s^{-1}.

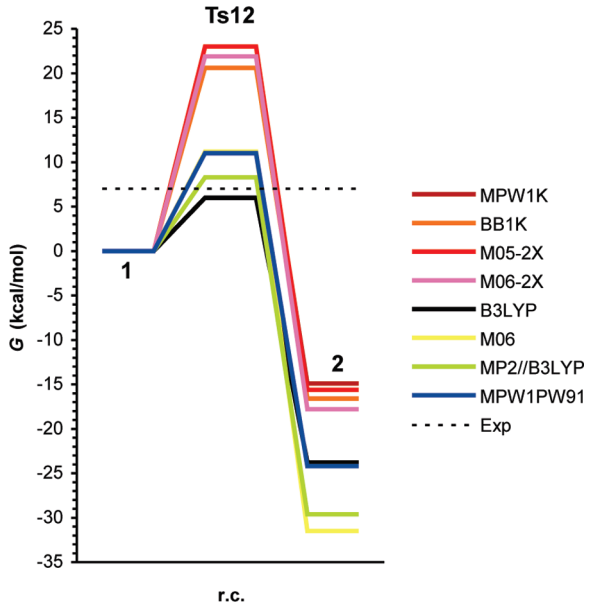

Figure 3. A reaction profile (ΔG) of the first redox step of GPX1 calculated with the MP2 and various DFT methods at the ONIOM-EE-QM/6-311+G(3df,2p):Amber//ONIOM-ME-DFT/6-31G(d,p):Amber level. $\Delta G_{exp}^{\ddagger}$ (dashed line) of 7 kcal mol^{-1} is estimated from k_{exp} = 4.1 × 10^7 M^{-1} s^{-1}.[4]

3.2. DFT Benchmark on Selenium Reactivity. We tested seven functionals for the structural prediction of transition states and reaction barriers. Two functionals fitted for thermochemical kinetics (MPW1K and BB1K) and new hybrid meta-GGA functionals (M05-2X,[36] M06-2X,[37] and M06[37]), which all have an average error on the reaction barriers in kinetics benchmarks[34−37,44−47] less than 2 kcal mol^{-1}, together with the MPW1PW91[32,33] functional used for modeling redox reactivity of selenium compounds with the SAPE mechanism[12−15] and with the B3LYP[30,31] functional used for the modeling of the redox cycle of GPX3[16,17] were applied. The MPW1PW91 and B3LYP functionals were less accurate in benchmarks on thermochemical kinetics parameters, and they underestimated the reaction barriers ca. 3−5 kcal mol^{-1}, from which MPW1PW91 performs slightly better.[34−37,44−47]

As can be seen in Table 1 [ONIOM-ME-DFT/6-31G(d,p):Amber] the most important structural parameters, the distances $d(Se^5-O^1)$ and $d(O^1-O^2)$, differ in the transition state more significantly for the $d(Se^5-O^1)$ (0.007−0.213 Å) and less apparently for the $d(O^1-O^2)$ (0.016−0.068 Å). The functionals with a smaller portion of the Hartree−Fock (HF) exchange (25%, MPW1PW91; 27%, M06 and 20%, B3LYP) predicted an earlier transition state, i.e., with the longer $d(Se^5-O^1)$ and shorter $d(O^1-O^2)$ distances compared with others (MPW1K, BB1K, M05-2X, and M06-2X; 42−56% of the HF exchange). For such TS geometries the reaction barriers in a large range of 13−28 kcal mol^{-1} [$\Delta G^{\ddagger}$, ONIOM-ME-DFT/6-31G(d,p):Amber] were found (Table 2). The results calculated with MPW1K, BB1K, M05-2X, and M06-2X converged to each other with $\Delta G^{\ddagger}$ = 27−28 kcal mol^{-1} and ΔG_r = −50 to −55 kcal mol^{-1}. The MPW1PW91, M06, and B3LYP predicted reaction barriers with significantly lower values of 17.0, 18.6, and 13.0 kcal mol^{-1} and comparable reaction energies of −50.6, −60.4, and −53.3 kcal mol^{-1} with the other DFT methods. The relatively high values of $\Delta G^{\ddagger}$ for the enzymatic chemical step predicted by the former functionals were further validated using more flexible basis set. When the 6-311+G(3df,2p) basis set was applied on the 6-31G(d,p) optimized structures, a dramatic decrease of the reaction barrier by about

Table 2. Relative Gibbs Free Energies (ΔG) Calculated for the Optimized Transition States and Intermediates at the Various DFT Levels [a]

ONIOM-ME[b]	B3LYP	MPW1PW91	MPW1K	BB1K	M05-2X	M06-2X	M06
1	0.0	0.0	0.0	0.0	0.0	0.0	0.0
TS12	13.0 (286i)	17.03 (355i)	27.1 (481i)	26.8 (461i)	28.2 (499i)	28.3 (490i)	18.6 (405i)
2	−53.3	−50.6	−51.9	−54.1	−50.4	−54.9	−60.4
ONIOM-ME[c]	B3LYP	MPW1PW91	MPW1K	BB1K	M05-2X	M06-2X	M06
1	0.0	0.0	0.0	0.0	0.0	0.0	0.0
TS12	10.3	14.4	24.1	22.5	23.7	22.8	13.5
2	−57.0	−56.6	−56.9	−59.5	−56.6	−60.4	−69.8
ONIOM-ME[c]	M06[d]	M06[e]	M06[f]	MP2[g]	MP2[h]	MP2[i]	
1	0.0	0.0	0.0	0.0	0.0	0.0	
TS12	13.8	13.7	9.3	13.8	12.0	10.9	
2	−66.3	−67.6	−69.2	−62.2	−64.9	−67.8	

[a] Using the ONIOM-ME-DFT/6-31G(d,p):Amber methodology (in kcal mol^{-1}), single point calculations energies with the 6-311+G(3df,2p) basis set applied with the MP2 and DFT methods, and imaginary vibrational frequencies (values in round brackets) for the transition states ($\nu^{\ddagger}$, in cm^{-1}). [b] ONIOM-ME-DFT/6-31G(d,p):Amber. [c] ONIOM-ME-QM/6-311+G(3df,2p):Amber//ONIOM-ME-DFT/6-31G(d,p):Amber. [d] M06//B3LYP. [e] M06//MPW1PW91. [f] M06//M06-2X. [g] MP2//B3LYP. [h] MP2//MPW1PW91. [i] MP2//MPW1K.

Table 3. Single Point Energy Calculations of Relative Gibbs Free Energies (ΔG) Calculated at the MP2 and Various DFT Levels[a]

ONIOM-EE	B3LYP	MPW1PW91	MPW1K	BB1K	M05-2X	M06-2X	M06
1	0.0	0.0	0.0	0.0	0.0	0.0	0.0
TS12	6.0	11.0	21.9	20.6	23.0	21.9	11.2
2	−23.8	−24.2	−14.9	−16.6	−15.6	−17.8	−31.5

ONIOM-EE	M06[b]	M06[c]	M06[d]	MP2[e]	MP2[f]	MP2[g]
1	0.0	0.0	0.0	0.0	0.0	0.0
TS12	9.6	10.8	9.6	8.3	8.4	9.6
2	−34.8	−34.8	−26.7	−29.6	−32.7	−25.8

[a] Using the ONIOM-EE-QM/6-311+G(3df,2p):Amber scheme (in kcal mol^{-1}). [b] M06//B3LYP. [c] M06//MPW1PW91. [d] M06//M06-2X. [e] MP2//B3LYP. [f] MP2//MPW1PW91. [g] MP2//MPW1K.

3−5 kcal mol^{-1} to values of 10−23 kcal mol^{-1} was found (Table 2). This indicates that at least medium-size basis set augmented by diffuse functions should be used for more accurate prediction for the kinetics parameters of the GPX-like systems. The differences in the prediction of the reaction barrier by the B3LYP, MPW1PW91, and M06 functionals are still extremely high (more than 8 kcal mol^{-1}) compared to the MPW1K, BB1K, M05-2X, and M06-2X functionals. The MPW1PW91 functional predicted the barrier (14.4 kcal mol^{-1}) in the best agreement with the MP2 method (12.0 kcal mol^{-1}, MP2//MPW1PW91), which was used as a reference QM method. The MPW1PW91 functional was also used by Bayse and Antony[12−15] for modeling redox reactivity of selenium compounds and showed the best performance in a DFT benchmark[14] on the reaction barriers of the redox reaction of methaneselenol with hydroperoximethane via the SAPE mechanism. The reaction barrier for reduction of hydrogen peroxide by selenocysteine and methaneselenol in their selenolate forms in gas phase, and an aqueous solution with a height of 15−21 kcal mol^{-1} was also predicted by MP2 and QCISD(T) methods.[19,21]

To evaluate electrostatic effects of enzyme surrounding and water environment on the reactivity of Sec45, the ONIOM methodology with electronic embedding was used [ONIOM-EE-DFT/6-311+G(3df,2p):Amber//ONIOM-ME-DFT/6-31G-(d,p):Amber]. The ONIOM-EE methodology together with the MPW1PW91, M06, and B3LYP functionals further decrease the reaction barrier ca. 2−4 kcal mol^{-1} to values of 11.0, 11.2, and 6.0 kcal mol^{-1}, indicating the importance of electrostatic effects of the enzyme (Table 3). However, for other functionals the ONIOM-EE barrier decreases only ca. 1−2 kcal mol^{-1}, predicting still high activation energies (22−23 kcal mol^{-1}) compared with the experimentally measured rate constant[4] of 4.1 × 10^{7} M^{-1} s^{-1} (Figure 3). We conclude that the MPW1PW91, M06, and B3LYP functionals predict the activation energies in the best agreement with the experimental results (estimated $\Delta G^{\ddagger}_{exp}$ is ca. 7 kcal mol^{-1}) and with our reference MP2 calculations (8.3−9.6 kcal mol^{-1}, Table 3). The other DFT methods, which have the higher portion of the HF exchange, seem to overestimate the reaction barrier for the first redox step of the GPX1 cycle by at least 10 kcal mol^{-1}. When the new hybrid meta-GGA M06 functional, with a similar portion of the HF exchange as MPW1PW91 and B3LYP have, was applied changing M06-2X (54% HF) with M06 (27% HF),[37] the reaction barrier dramatically decreases from 21.9 to 9.6−11.2 kcal mol^{-1} (Table 3, M06, M06//M06-2X, M06//B3LYP, and M06//MPW1PW91). The M06 values are now very close to the MPW1PW91 and MP2 results.

4. CONCLUSION

Using the QM/MM methodology in this work as well as the MD simulations and pK_a calculations in the previous work,[11] we demonstrated that the ionized selenolate state of Sec45 in GPX1 is the favorable form for the reduction of hydroperoxide substrates. The efficient reduction of hydroperoxides by GPX1 can only proceed in the enzyme environment, with a general acid/base catalyst which directly participates in proton exchange with the substrate. Such a role could play a weak acid or base, i.e., the catalyst with pK_a > 7. In GPX1 it could be Arg177. The GPX1-Se^{-}-Arg177H^{+} mechanism has the activation barrier of 6−11 kcal mol^{-1} consistent with the experimentally measured rate constant for the first redox step of GPX1[4] and is 2−3 times lower compared with those calculated for the GPX3-Se^{-}-H_2O-Gln83H^{+},[16] the GPX3-SeH-Gln83[17] of glutathione peroxidase from class 3, and the SAPE mechanism[12−15] of GPX-like organoselenium compounds. The acidic strength and the proper position of the catalytic acid/base in the active-site for direct proton exchange with the hydroperoxide substrate seem to be crucial factors for a rate of ca. 10^{7} M^{-1} s^{-1} of the redox enzymatic reaction. This can explain why the QM calculations[19] on the redox reaction of selenocysteine without the assistance of the proton exchange catalyst predicted the higher reaction barrier corresponding to a slow chemical process of a rate of ca. 0.25 M^{-1} s^{-1}.

Our DFT benchmark calculations indicate that for the more accurate prediction of the selenium reactivity, at least a medium-size basis set augmented by diffuse function and proper description of surrounding electrostatic effects are required. The DFT methods, which were designed for kinetics (MPW1K and BB1K) as well as the new Minnesota functionals with double the amount of nonlocal exchange (M05-2X and M06-2X), all with a higher portion of the HF exchange, seem to significantly overestimate the reaction barrier for GPX1 by more than 10.0 kcal mol^{-1} compared with the experimental results,[4] the MP2 method, or with the MPW1PW91, M06, and B3LYP functionals. We recommend for modeling the selenium reactivity the functionals with a lower portion of the HF exchange.

■ ASSOCIATED CONTENT

Supporting Information. Total and relative electronic energies, thermal corrections to Gibbs free energies, force field parameters used for the Sec45 residue and H_2O_2, and Gaussian input files of the MPW1PW91 optimized structures. This information is available free of charge via the Internet at http://pubs.acs.org/.

AUTHOR INFORMATION

Corresponding Author
*E-mail: chemkona@savba.sk. Telephone: +421-2-59410322.

ACKNOWLEDGMENT

Financial support for this research was granted by the Scientific Grant Agency of the Ministry of Education of Slovak Republic and Slovak Academy of Sciences (project VEGA-02/0176/09), the Slovak Research and Development Agency (project APVV-0117-06), the Austrian Federal Ministry of Science and Research (Action Austria-Slovakia, ICM-2010-02933), and the European Community's Seventh Framework Programme (FP7/2007-2013) under grant agreement no. 212043.

REFERENCES

(1) Flohé, L.; Gunzler, W. A.; Schock, H. H. *FEBS Lett.* **1973**, *32*, 132.
(2) Epp, O.; Ladenstein, R.; Wendel, A. *Eur. J. Biochem.* **1983**, *133*, 51.
(3) Gettins, P.; Crews, B. C. *J. Biol. Chem.* **1991**, *266*, 4804.
(4) Takebe, G.; Yarimizu, J.; Saito, Y.; Hayashi, T.; Nakamura, H.; Yodoi, J.; Nagasawa, S.; Takahashi, K. *J. Biol. Chem.* **2002**, *277*, 41254.
(5) Roy, G.; Nethaji, M.; Mugesh, G. *J. Am. Chem. Soc.* **2004**, *126*, 2712.
(6) Kavanagh, K. L.; Johansson, C.; Smee, C.; Gileadi, O.; Von Delft, F.; Weigelt, C. J.; Sundstrom, M.; Edwards, A.; Oppermann, U. *Crystal Structure of the Selenocysteine to Glycine Mutant of Human Glutathione Peroxidase 1*; The Research Collaboratory for Structural Bioinformatics (RCSB) : RCSB-Rutgers, RCSB-San Diego Supercomputer Center, and RCSB-University of Wisconsin-Madison; http://www.rcsb.org/. Accessed December 09, 2010; PDB ID: 2F8A.
(7) Ren, B.; Huang, W. H.; Akesson, B.; Ladenstein, R. *J. Mol. Biol.* **1997**, *268*, 869.
(8) Dimastrogiovanni, D.; Anselmi, M.; Miele, A. E.; Boumis, G.; Petersson, L.; Angelucci, F.; Di Nola, A.; Brunori, M.; Bellelli, A. *Proteins* **2010**, *78*, 259.
(9) Alphey, M. S.; Konig, J.; Fairlamb, A. H. *Biochem. J.* **2008**, *414*, 375.
(10) The Research Collaboratory for Structural Bioinformatics: : RCSB-Rutgers, RCSB-San Diego Supercomputer Center, and RCSB-University of Wisconsin-Madison; http://www.rcsb.org/. Accessed December 09, 2010; PDB ID: 2R37, 2P31, 2I3Y, 2HE3, 2G3S, 3CYN.
(11) Ali, S. T.; Jahangir, S.; Karamat, S.; Fabian, W. M. F.; Nawara, K.; Kóňa, J. *J. Chem. Theory Comput.* **2010**, *6*, 1670.
(12) Bayse, C. A. *J. Phys. Chem. A* **2007**, *111*, 9070.
(13) Bayse, C. A.; Antony, S. *J. Phys. Chem. A* **2009**, *113*, 5780.
(14) Bayse, C. A.; Antony, S. *Main Group Chem.* **2007**, *6*, 185.
(15) Bayse, C. A. *J. Inorg. Biochem.* **2010**, *104*, 1.
(16) Prabhakar, R.; Vreven, T.; Morokuma, K.; Musaev, D. G. *Biochemistry* **2005**, *44*, 11864.
(17) Prabhakar, R.; Vreven, T.; Frisch, M. J.; Morokuma, K.; Musaev, D. G. *J. Phys. Chem. B* **2006**, *110*, 13608.
(18) Prabhakar, R.; Musaev, D. G.; Khavrutskii, I. V.; Morokuma, K. *J. Phys. Chem. B* **2004**, *108*, 12643.
(19) Cardey, B.; Enescu, M. *J. Phys. Chem. A* **2007**, *111*, 673.
(20) Kóňa, J.; Brinck, T. *Org. Biomol. Chem.* **2006**, *4*, 3468.
(21) Cardey, B.; Enescu, M. *ChemPhysChem* **2005**, *6*, 1175.
(22) Bachrach, S. M.; Walker, C. J.; Lee, F.; Royce, S. *J. Org. Chem.* **2007**, *72*, 5174.
(23) Bachrach, S. M.; Demoin, D. W.; Luk, M.; Miller, J. V. *J. Phys. Chem. A* **2004**, *108*, 4040.
(24) Benková, Z.; Kóňa, J.; Gann, G.; Fabian, W. M. F. *Int. J. Quantum Chem.* **2002**, *90*, 555.
(25) Pearson, J. K.; Boyd, R. J. *J. Phys. Chem. A* **2006**, *110*, 8979.
(26) Pearson, J. K.; Boyd, R. J. *J. Phys. Chem. A* **2007**, *111*, 3152.
(27) Li, H.; Robertson, A. D.; Jensen, J. H. *Proteins* **2005**, *61*, 704.
(28) Vreven, T.; Byun, K. S.; Komáromi, I.; Dapprich, S.; Montgomery, J. A., Jr.; Morokuma, K.; Frisch, M. J. *J. Chem. Theory Comput.* **2006**, *2*, 815.
(29) Frisch, M. J.; Trucks, G. W.; Schlegel, H. B.; Scuseria, G. E.; Robb, M. A.; Cheeseman, J. R.; Scalmani, G.; Barone, V.; Mennucci, B.; Petersson, G. A.; Nakatsuji, H.; Li, X.; Hratchian, H. P.; Izmaylov, A. F.; Bloino, J.; Zheng, G.; Sonnenberg, J. L.; Hada, M.; Ehara, M.; Toyota, K.; Fukuda, R.; Hasegawa, J.; Ishida, M.; Nakajima, T.; Honda, Y.; Kitao, O.; Nakai, H.; Vreven, T.; Montgomery, J. A., Jr.; Peralta, J. E.; Ogliaro, F.; Bearpark, M.; Heyd, J. J.; Brothers, E.; Kudin, K. N.; Staroverov, V. N.; Kobayashi, R.; Normand, J.; Raghavachari, K.; Rendell, A.; Burant, J. C.; Millam, J. M.; Iyengar, S. S.; Tomasi, J.; Cossi, M.; Scalmani, G.; Rega, N.; Millam, J. M.; Klene, M.; Knox, J. E.; Cross, J. B.; Bakken, V.; Adamo, C.; Jaramillo, J.; Gomperts, R.; Stratmann, R. E.; Yazyev, O.; Austin, A. J.; Cammi, R.; Pomelli, C.; Ochterski, J. W.; Martin, R. L.; Morokuma, K.; Zakrzewski, V. G.; Voth, G. A.; Salvador, P.; Dannenberg, J. J.; Dapprich, S.; Daniels, A. D.; Farkas, O.; Foresman, J. B.; Ortiz, J. V.; Cioslowski, J.; Fox, D. J. *Gaussian 09*, revision A.02; Gaussian, Inc.: Wallingford, CT, 2009.
(30) Becke, A. D. *J. Chem. Phys.* **1993**, *98*, 5648.
(31) Lee, C. T.; Yang, W. T.; Parr, R. G. *Phys. Rev. B* **1988**, *37*, 785.
(32) Adamo, C.; Barone, V. *J. Chem. Phys.* **1998**, *108*, 664.
(33) Perdew, J. P.; Burke, K.; Wang, Y. *Phys. Rev. B* **1996**, *54*, 16533.
(34) Lynch, B. J.; Fast, P. L.; Harris, M.; Truhlar, D. G. *J. Phys. Chem. A* **2000**, *104*, 4811.
(35) Zhao, Y.; Lynch, B. J.; Truhlar, D. G. *J. Phys. Chem. A* **2004**, *108*, 2715.
(36) Zhao, Y.; Schultz, N. E.; Truhlar, D. G. *J. Chem. Theory Comput.* **2006**, *2*, 364.
(37) Zhao, Y.; Truhlar, D. G. *Theor. Chem. Acc.* **2008**, *120*, 215.
(38) Frisch, M. J.; Head-Gordon, M.; Pople, J. A. *Chem. Phys. Lett.* **1990**, *166*, 275.
(39) Møller, C.; Plesset, M. S. *Phys. Rev.* **1934**, *46*, 618.
(40) Cheatham, T. E.; Cieplak, P.; Kollman, P. A. *J. Biomol. Struct. Dyn.* **1999**, *16*, 845.
(41) Jorgensen, W. L.; Chandrasekhar, J.; Madura, J. D.; Impey, R. W.; Klein, M. L. *J. Chem. Phys.* **1983**, *79*, 926.
(42) Roothaan, C. C. J. *Rev. Mod. Phys.* **1951**, *23*, 69.
(43) Singh, U. C.; Kollman, P. A. *J. Comput. Chem.* **1984**, *5*, 129.
(44) Zhao, Y.; Pu, J. Z.; Lynch, B. J.; Truhlar, D. G. *Phys. Chem. Chem. Phys.* **2004**, *6*, 673.
(45) Zhao, Y.; Gonzalez-Garcia, N.; Truhlar, D. G. *J. Phys. Chem. A* **2005**, *109*, 2012.
(46) Sousa, S. F.; Fernandes, P. A.; Ramos, M. J. *J. Phys. Chem. A* **2007**, *111*, 10439.
(47) Zhao, Y.; Truhlar, D. G. *J. Phys. Chem. A* **2005**, *109*, 5656.
(48) Byun, B. J.; Kang, Y. K. *Biopolymers* **2011**, *95*, 345.
(49) Goto, K.; Nagahama, M.; Mizushima, T.; Shimada, K.; Kawashima, T.; Okazaki, R. *Org. Lett.* **2001**, *3*, 3569.
(50) Back, T. G.; Dyck, B. P. *J. Am. Chem. Soc.* **1997**, *119*, 2079.